PHYSICAL REVIEW B VOLUME 16, NUMBER 9 1 NOVEMBER 1977

Distribution of irradiation damage in silicon bombarded with hydrogen

W. K. Chu, R. H. Kastl, R. F. Lever, S. Mader, and B. J. Masters
IBM System Products Division, East Fishkill, Hopewell Junction, New York 12533
(Received 24 May 1977)

Damage distribution in [001] silicon crystals bombarded with a fluence of $10^{16}/cm^2$ to $10^{17}/cm^2$ H^+ ions at 50–250 keV and at implantation temperatures from −170 to 600°C was measured by use of high-energy $^4He^+$ channeling. The depth profiles were verified by spreading-resistivity measurements, by radiation-enhanced diffusion measurements, and by sectioning of a sample on which blisters had formed. The hydrogen profile, measured by $^{15}N(p,\alpha\gamma)^{12}C$ reaction, agrees with the damage distribution. For 200 keV the depth measurements agree with values calculated by theoretical methods, and the depth distribution is 30%–60% narrower.

I. INTRODUCTION

In studies of ion implantation in silicon, the common practice has been to use active ions such as boron, phosphorus, and arsenic to tailor the electrical properties, and to use silicon ions or heavy-inert-gas ions such as argon and krypton to create radiation damage. Very little attention has been given to hydrogen implantation in silicon. Recently, the implantation of hydrogen and helium in metals has received increasing attention.[1,2] It has found application in the simulation of controlled thermonuclear reaction environments; also, radiation-enhanced diffusion[3] and shallow donor formation[4] due to proton bombardment have shown potential for application in fabricating semiconductor devices. Theoretical and experimental work on hydrogen implantation in solids becomes crucial to these applications.

Recently Thompson and Robinson[5] used channeled backscattering in studying damage distributions for ions implanted in silicon at energies of 10–40 keV and a temperature of 45 °K. They compared their damage measurement with a Monte Carlo calculation and found that the electronic stopping cross section is 60% higher than the standard calculation based on Lindhard, Scharff, and Schiøtt (LSS).

Ligeon and Guivarc'h[6] studied hydrogen implanted at 1.5–60 keV. They measured the range distribution of hydrogen by the $^1H(^{11}B,\alpha)\alpha\alpha$ nuclear reaction, and the damage profile by channeling and backscattering of 1.5-MeV ^4He ions. They concluded that the hydrogen distribution and the damage profile are very similar.

We have briefly reported radiation damage done to silicon by bombardment with 50–250-keV hydrogen; the study was made chiefly by transmission-electron microscopy.[7] In this paper, we will study damage distribution by channeling; the use of this method will be justified, and the results will be compared with those obtained by theoretical calculations.

II. IMPLANTING THE HYDROGEN IONS

All of the hydrogen ions were implanted with a 500-kV Van de Graaff accelerator (HVEC Model K-501). The accelerating voltage was calibrated for $^{11}B(p,\gamma)$ at 163.1 keV,[8] for $^{14}N(p,\gamma)$ reactions at 278.1 keV,[9] and for $^{19}F(p,\alpha\gamma)$ at 340.4 keV.[10] The uncertainty of the implantation energy was within ±1 keV. The energy stability of the ion beam was governed by a generating voltmeter and/or a feedback slit arrangement following the analyzing magnet. An electrostatic scanner was used to provide a beam raster over the target area. Neutrals were removed from the ion beam by installing a 3° bend in the flight tube and applying the appropriate dc bias to the horizontal scanning plates. The vacuum in the beam line and target chamber was 4×10^{-6} Torr. The target chamber was constructed so that, whether a cold stage or a medium-temperature furnace was attached, the wafer position would remain constant relative to a beam-defining mask. The cold stage consisted of a wafer holder (copper) attached to a 0.75-in.-diam copper rod through an insulated vacuum seal. Cooling the copper rod with liquid nitrogen made it possible to keep the temperature of the wafer holder at 120 °K, measured with an iron-constantan thermocouple. Dow-Corning vacuum grease was used for the thermal contact.

For all implants done at room temperature and above, a tube furnace 18 in. long and 4 in. in diameter was used. The heating element was 0.030-in. tantalum wire wrapped on a quartz tube and covered with a second quartz tube. The heat shields and reflectors were made from 0.005-in. stainless steel. Temperatures of at least 980 °C could be obtained; they were measured with a

Copyright © 1977 by The American Physical Society

chromel-alumel thermocouple and/or an Ircon Infrared Radiation Thermometer, Series 7000, with probable errors of ±5 °C at low temperature and ±20 °C at high.

p-type silicon wafers, 0.015 in. thick and with a resistivity of 10–20 Ω cm, were cut 1.5° off the ⟨100⟩ axis. All the wafers were from the same lot. During implantation, to minimize channeling, they were tilted 7° off normal incidence. The total beam current and the ion fluence at the wafer surface were monitored by a BIC Current Integrator, Model 1000 C. Both the uncertainty of the ion fluence and that of the implantation uniformity were established to be about ±5%. The dose of implantation ranged from $10^{16}/cm^2$ to $2 \times 10^{17}/cm^2$; for most of the study, however, a dose of $4 \times 10^{16}/cm^2$ was used.

III. DAMAGE DISTRIBUTION IN HYDROGEN-BOMBARDED SILICON

We approached the damage distribution by various methods. Most of the measurements were made by backscattering and channeling to profile the defect distribution due to hydrogen bombardment. The results were verified by profiling the hydrogen distribution with nuclear reaction, by measuring the depths of blisters, and by spreading-resistance measurement on a beveled sample. In the following sections we will discuss these various methods and the results obtained with each.

A. Measurement by backscattering and channeling

Damage distribution for protons in silicon was measured by backscattering and channeling with $^4He^+$ ions at 1.0–2.8 MeV. Most of the data were taken at 2.4 MeV ^4He, with a current of 20–40 nA, and a beam spot of 0.5 mm^2. The silicon sample was mounted on a goniometer that had three degrees of freedom: rotation, tilt, and translation. The beam was aligned with respect to the ⟨100⟩ axis at the center part of the target, where an area 2 mm in radius had been etched to expose the undamaged silicon to the analyzing beam. After the beam was aligned on this center part, the target was translated by about 4 mm so that the proton-damaged region was under investigation. A random spectrum was obtained by tilting the target by 7° and rotating the target during the run, or alternatively at a fixed angle such as 7° from the ⟨100⟩ axis and 10° from the {110} plane.

A typical set of runs is given in Fig. 1, for samples damaged by $4 \times 10^{16}/cm^2$ protons at 85, 125, 175, and 200 keV at room temperature. For the data acquisition, 10 μC of 2.4-MeV helium ions backscattered at 170 °C with incidence along the ⟨100⟩ direction was used, and the solid angle for

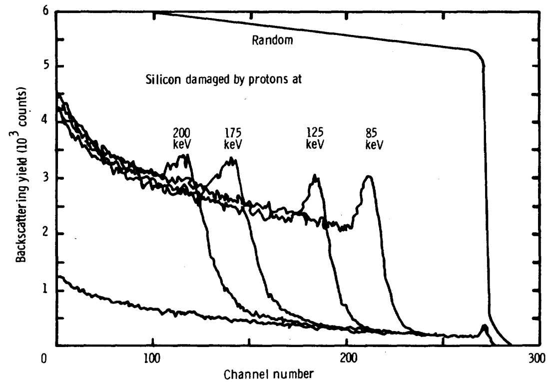

FIG. 1. Channeled backscattering spectra of 2.4-MeV He^+ from silicon bombarded with 4×10^{16} H^+/cm^2 at room temperature.

the scattering was 4.11 msr. The damage region is seen to be well localized at a given depth, and in the surface region of the sample the amount of damage is too small to be detected by channeling.

Every spectrum contains contributions from both scattering and dechanneling. To extract the damage profile, the contributions must be separated; that is, the dechanneling background must be obtained beneath the damage spectrum. Ziegler[11] and Schmid[12] treated this type of problem by the method of Bøgh.[13] Both their treatments require that a dechanneling model be assumed. It turns out that if the damage peak is large by comparison to the dechanneling contribution, the uncertainty in dechanneling background does not significantly influence either the position of the damage peak or the full width at half maximum (FWHM) of the damage spectrum.

For our analysis we modify Ziegler's method[11] by combining single scattering and multiple scattering in the dechanneling calculation. The calculation begins with a dechanneling level for a ^4He beam traversing an undamaged crystal. Any increase in the random fraction of the yield is assumed to be due to scattering from "displaced silicon atoms," and the dechanneling due to those "displaced atoms" is calculated; the amount of random fraction of the yield due to dechanneling is then subtracted for this depth and the next depth interval. The number of "equivalent displaced atoms" and their dechanneling contribution are calculated again. The procedure is continued for increasing depth until the defect-free region is reached, and then the depth distribution of the displaced atoms is obtained.

Figure 2 shows damage distributions obtained by applying this procedure to the energy spectra in Fig. 1. No correction is made for the resolution of the detecting system or for energy straggling of helium ions in silicon. Such effects lead to a cor-

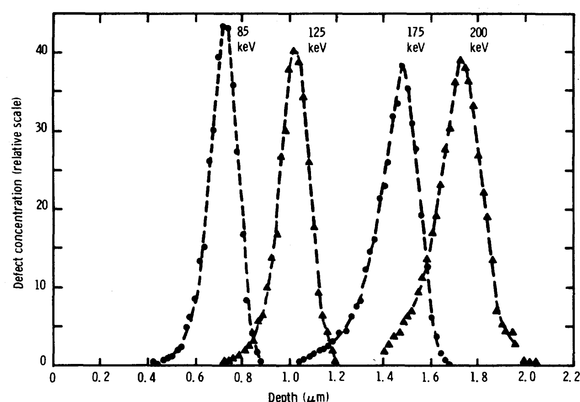

FIG. 2. Defect distribution, extracted from Fig. 1. Defect concentration is expressed as the equivalent silicon atoms displaced from the lattice site, expressed as percentage of silicon atoms randomly displaced.

rection of 20–40 Å to the broadening of the FWHM of the extracted profile given in Fig. 2. Those corrections are made to all extracted profiles to yield the final result.

The defect concentration given in Fig. 2 is on a relative scale. If one translates the concentration into the equivalent number of random scattering atoms that produces the random peak and the dechanneling level given in Fig. 1, the relative scale in Fig. 2 can be considered to be the percentage of the silicon atoms randomly displaced from the lattice site. Near the maximum defect region, for example (Fig. 2), the fact that about 40% of the silicon atoms are randomly distributed off lattice site is what produces the dechanneling spectrum given in Fig. 1.

The depth scale is obtained by using the energy-loss table of Ziegler and Chu.[14] For the incident part of the beam, channel energy loss along the ⟨100⟩ direction is assumed to be 80% of the value for random direction. Any localized energy-loss value is a superposition of channeled and random energy loss according to the fractional amount of random atoms in silicon crystal. One can easily see in Fig. 1 that the area in front of the defect region is almost free of damage.

The ±5% uncertainty in the energy loss will influence the depth scale directly. The uncertainty in the ratio of ⟨100⟩ energy loss to random energy loss will influence it less. For example, changing this ratio from 0.6 to 1.0 (instead of 0.8, the value used in our calculation) will increase or decrease the depth by only 5%, because the outgoing path is along a random direction.

B. Tests of backscattering and channeling procedure

In extracting a damage profile from the channeling spectrum, two assumptions are made: (i) that scattering and dechanneling by defects can be expressed as coming from randomly displaced silicon atoms at a given depth, and (ii) that the defect distribution is identical with the damage energy distribution, with no complication by long-range migration or diffusion. Both of these assumptions need to be explained and justified. We will elaborate on them, and demonstrate with reference to special cases when either assumption breaks down.

It is well known[15] that a channeled backscattering measurement can produce only an indication about the degree of lattice disorder, not the number of "displaced atoms." In the dechanneling calculation, however, for convenience in extracting profiles, we have treated both scattering and its dechanneling efficiency due to defects as resulting from "randomly displaced atoms." We have the boundary condition that after the ion beam passes the defect region, the amount of dechanneling, calculated on the basis of randomly displaced scattering centers, should reach a level that agrees with the experimental dechanneled spectrum. Randomly displaced atoms produce a well-defined dechanneling-to-scattering ratio. If a certain kind of defect is more effective in dechanneling than in scattering, this ratio will be different. Let us define the ratio for randomly displaced atoms, divided by the ratio for the defect, as the relative dechanneling factor ϵ. Then ϵ can be used in the calculation to force agreement between the calculated spectrum and the spectrum beneath the damaged region. When $\epsilon = 1$, the defects produce scattering and dechanneling equivalent to that from randomly displaced atoms, and no correction is actually made. When $\epsilon > 1$, the defects are more effective at dechanneling (or less effective in scattering) than randomly displaced atoms. Implantation at different temperatures produces different defects,[7] which in turn produce different values of ϵ. A measurement of ϵ versus implantation temperature for 50-keV hydrogen atoms in a dose of $4\times10^{16}/cm^2$ is given in Fig. 3. Also given there is the total amount of dechanneling, defined as the ratio of the heights of the two spectra, channeled and random, right beneath the damage peak. For implantation at temperatures from −200 to 0 °C or above 460 °C, the total amount of dechanneling is smaller. Further, ϵ stays near unity for temperatures up to 440 °C; at temperatures above 500 °C, however, primarily because defects produced at these temperatures lead to much less scattering, ϵ increases to 4.

As was mentioned earlier, ϵ is defined as a measurement of the dechanneling ability of a given defect distribution as compared with the dechanneling ability of silicon atoms randomly distributed inside a silicon crystal. The reduction of total de-

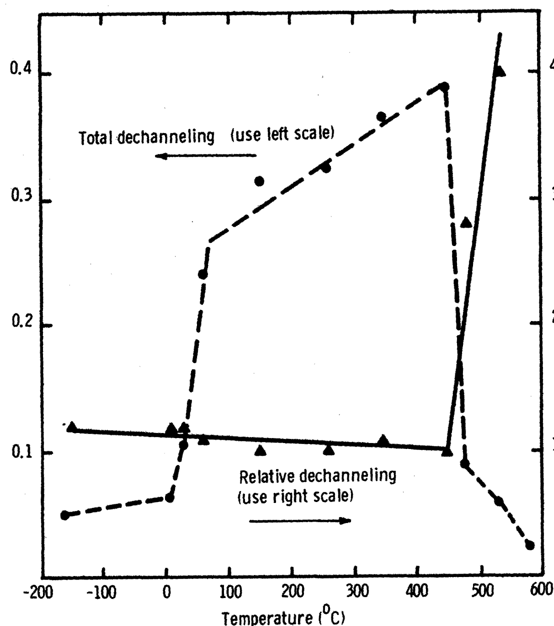

FIG. 3. Total and relative dechanneling due to defects as a function of ambient temperature. Total dechannel is a direct measurement of the dechanneling level right beneath the damage region of the spectrum. Relative dechanneling ϵ is a parameter used in the extraction of defect distribution (see text).

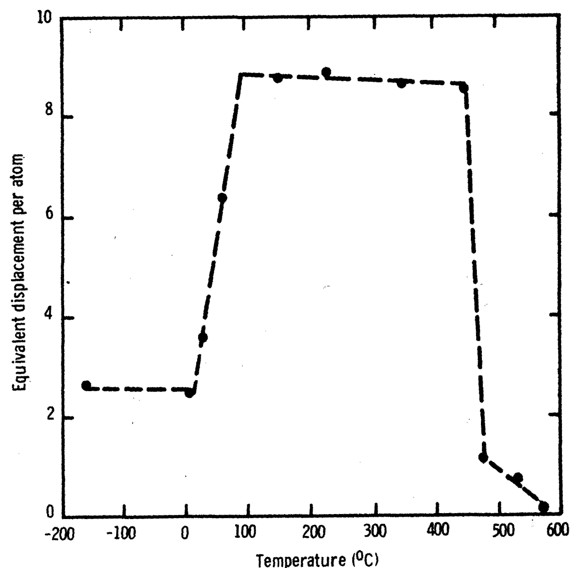

FIG. 4. Total amount of defect expressed as the equivalent silicon atoms displacement per incident proton, as a function of implantation temperature.

channeling (dashed curve in Fig. 3) at low or very high temperatures is due to a reduction in the total amount of damage—a reduction that is not well understood. One possible explanation is that most of the atomic displacements produce closely separated Frenkel pairs. At low temperatures, the vacancies are relatively immobile and migration of the interstitials is limited to a few atomic jumps, so that eventually almost all of the original Frenkel pairs are annihilated by direct recombination. Above room temperature, the mean diffusion length of the interstitials becomes much larger; a few of them are therefore able to escape from the depth region at which they were generated, leaving behind a vacancy-rich region which manifests itself as observable damage. At temperatures approaching 500 °C, the excess vacancies too become mobile and coalesce at internal surfaces, thus reducing the amount of scattering observed and increasing the relative dechanneling factor. It is also possible that the vacancy-rich damaged region is stabilized by entrapped hydrogen up to about 500 °C, at which point the hydrogen begins to diffuse out,[16] and the crystal recovers.

The amount of damage in silicon, for 4×10^{16} protons/cm^2 implanted at 50 keV at various temperatures, is given in Fig. 4. The number of defects is measured from the total area under a channeled backscattering spectrum, where defects are considered to be randomly distributed atoms that produce the same channeling spectrum. This virtual number of displaced atoms is normalized to be implantation dose. Figure 4 indicates that for doses of $(1-8)\times10^{16}$ at most of the implantation temperatures, the defect formation is equivalent to 8 or 9 silicon atoms permanently displaced from the lattice site, per incident proton. At both low and high temperatures, the formation of permanent defects is reduced. The correlation of dechanneling with the nature of the defects observed by transmission-electron microscopy (TEM) has been studied. We have elaborated this correlation in an earlier paper,[7] in which we discuss the effect of ambient temperature on the nature of the damage.

In regard to the actual depth scale in a dechanneling measurement, Quere[15] has pointed out that in observations of the depth dependence of the defect profile, the dechanneling is seen to occur on or beyond the defect, if the defect is one, such as a stacking fault, whose chief effect is obstruction of the projectile. The dechanneling may occur either before or beyond the defect, if the defect—for example, a dislocation—distorts the lattice. In the first case the experimental profile will be both broader and deeper than the actual profile; in the second case, it is at least broader. Thus an understanding of the nature of the defect becomes crucial in interpreting the channeling spectrum. The perturbation distance involved in the above argument[15] is a depth of about one-quarter of the oscillation length of the probing projectile

in the crystal. For 2.4-MeV ^{4}He ions channeling along the ⟨100⟩ direction in silicon, we estimate this perturbation distance to be about 700 Å. The maximum perturbation in the depth and depth distribution, for 700-Å perturbation in dechanneling, is estimated to be less than 200 Å for our profile extraction method. Therefore, the maximum systematic error in our profile extraction, which is due to the above perturbation, would seem to be 200 Å.

We do not believe, however, that our profile extraction suffers such a systematic error, because we have subjected it to two tests that seem to indicate otherwise. First, we have studied the depth-profiles obtained at various ion energies, 1, 1.5, 2.0, 2.4, and 2.8 MeV. For all these energies, the depth profiles of hydrogen implanted at 50 keV at room temperature are essentially the same. This test shows that the damage profiles obtained by channeling and backscattering are self-consistent. The perturbation in distances due to dechanneling, discussed by Quere, is energy dependent.

The second test is performed on samples implanted at various ambient temperatures. If dechanneling perturbation influences the defect profiles we extract, this perturbation will be sensitive to the nature and size of the defect. Figures 5 and 6 show the defect depth and standard deviation of a silicon crystal bombarded with protons at 50 keV and various temperatures. Profiles are extracted from 2.4-MeV He channeling spectra. From Figs. 5 and 6 one can see that at higher temperatures the profile becomes shallower and broader. Also, as TEM study[7] shows, the defect grows in size and in distribution. Therefore, the change in defect profiles at higher temperature is due to the growth and migration of defects. At lower temperatures a unique profile can be obtained, which, as was mentioned earlier, is independent of probing energies. In studying the depth distribution of damage, most of the data are taken for doses implanted at temperatures from room temperature to 100 ℃, generated by beam heating. Depth and depth distribution are essentially the same as for low-temperature implants (Figs. 5 and 6); the relative dechanneling factor ϵ is within 15% of unity (Fig. 3), and the equivalent displacement per atom (Fig. 4) is large enough for sensitive profiling of damage.

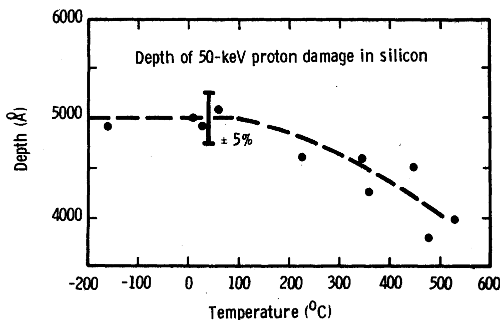

FIG. 5. Mean depth of the defect distribution in silicon damaged by protons at 50 keV, studied as a function of ambient temperature.

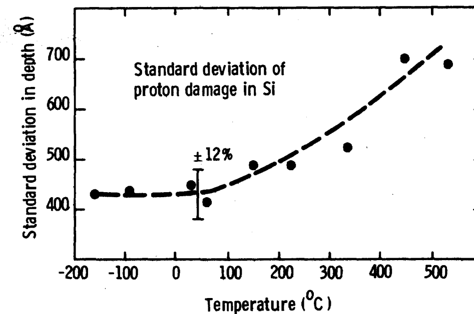

FIG. 6. Standard deviation of proton damage in silicon, studied as a function of temperature.

C. Hydrogen distribution by nuclear reaction

Hydrogen profiles can be obtained by a method, described by Lanford *et al.*,[17] that uses the resonance of nuclear reaction between protons and ^{15}N. This resonant reaction, $^{15}\mathrm{N}(p, \alpha\gamma)^{12}\mathrm{C}$, occurs at the center-of-mass energy 402 keV; it has a FWHM of 0.9 keV, and a peak cross section of 200 mb. To use this reaction as a probe for hydrogen, we bombard the hydrogen-embedded silicon with ^{15}N ions at 6.4–8 MeV. The γ-ray yield as a function of ^{15}N energy (Fig. 7) gives the depth distribution of hydrogen. In the laboratory sys-

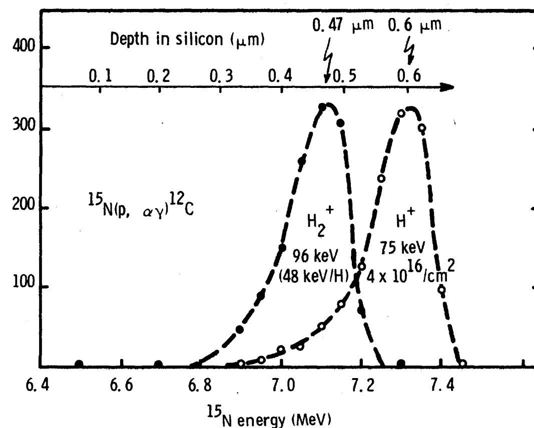

FIG. 7. Hydrogen profile obtained by nuclear reaction with a high-energy ^{15}N beam. The γ yield as a function of ^{15}N energy gives the depth distribution of hydrogen in silicon. Values of nitrogen energy loss in silicon from Northcliffe and Schilling are used in translating the energy scale into a depth scale.

tem, ^{15}N with an energy of 6.385 MeV, when incident on hydrogen, yields 4.43-MeV γ rays. When the hydrogen is embedded in a silicon target, the ^{15}N must have higher energy in order to induce the reaction, because it loses some energy in traversing the silicon before it reaches the hydrogen. To calculate the energy loss in the target, the tables of Northcliffe and Schilling can be used to convert the energy scale to the depth scale; both scales are given in Fig. 7. This method was applied to two silicon samples that had been implanted with hydrogen ions, one at 48 keV and the other at 75 keV. Both depth and depth distribution agreed within 4% with those for the damage profile.

Similar agreement was obtained by Ligeon and Guivarc'h,[6] who compared the damage profile with that of the hydrogen profile determined by the $^{1}H(^{11}B, \alpha)\alpha\alpha$ nuclear reaction.

D. Verification of depth profile by alternative methods

In addition to channeled ^{4}He backscattering and nuclear reaction, several other observations made in the course of our studies provide useful measurements of the projected range to which protons penetrate silicon.

When crystalline silicon at room temperature is bombarded at fluences of the order of 10^{17} protons/cm^2, the surface becomes "blistered," presumably because of the combined effects of (i) a high compressive strain in the lattice at the depth region, corresponding to maximum displacement damage, and (ii) the tendency of hydrogen atoms implanted in silicon at concentrations exceeding several atomic percent to agglomerate at high pressure, forming molecular hydrogen and possibly silane-related species. On further bombardment, or during subsequent annealing, these blisters erupt to form flat-bottomed craters. Figure 8 shows the beveled cross section of a ⟨100⟩-oriented wafer that had been implanted near room temperature with 2×10^{17}/cm^2 of protons at 150 keV and then annealed for 30 min at 900 ℃. Both unbroken blisters (about 10 μm in diameter) and the larger craters left by erupted blisters are evident. The crater depth obtained in this measurement, 1.30 μm, agrees reasonably well with the penetration range obtained by ion scattering. A similar measurement of crater depth, by use of optical interferometry, has been reported by Baruch *et al.*[18]

As protons in silicon lose energy by both ionization and the displacement process, the target material loses some electrical conductivity.[19] Figure 9(a) shows the spreading-resistance depth profile obtained from an unannealed 0.3-Ω cm n-type ⟨100⟩ wafer, beveled at 1°, after bombardment at room temperature with 5×10^{11}/cm^{-2} of 150-keV protons. The depth at which the conductivity loss reaches its maximum, about 1.2 μm, indicates that the loss is due to defects induced by displacement. The compensating defects and carrier mobility degradation that are introduced into this depth region are greatly reduced by post-bombardment annealing at 100 ℃. The proton ranges inferred from measurements of this type are slightly smaller than is indicated by the chan-

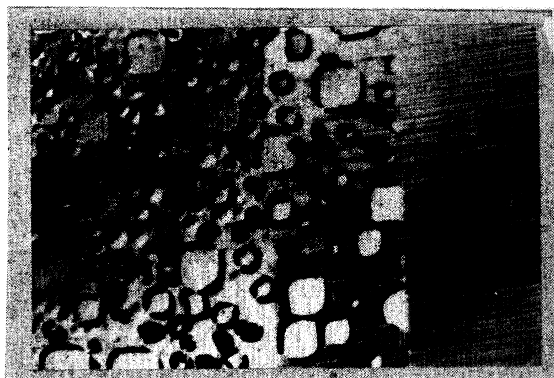

FIG. 8. Optical microscope view, showing the circular gas bubbles or blisters formed by high-dose proton bombardment in silicon, and the almost square craters that result from blister eruption in a ⟨100⟩ specimen. Magnification 700×. The crater depth can be determined from the length measurement and the beveling angle.

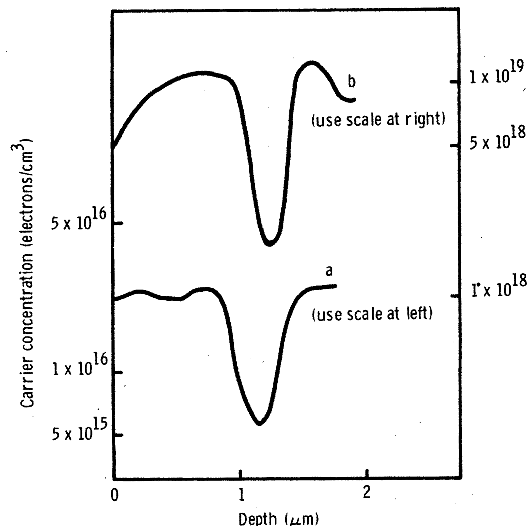

FIG. 9. Results of spreading-resistance measurements on beveled samples. (a) Lower curve: The loss of electrical conductivity due to proton bombardment gives the depth profile. (b) Upper curve: Arsenic concentration profile measured after 150-keV proton bombardment at 700 °C and post-bombardment annealing at 900 °C in Ar. The dopant rejection at 1.2μm is due to radiation-enhanced diffusion.

neling data given above, possibly owing to a contribution from shallow donor activity[20] of the implanted hydrogen.

Yet another indication of proton penetration in silicon is provided by measurements of the impurity redistribution that takes place during high-temperature bombardment with protons. As Baruch *et al.* first observed, boron is preferentially rejected from the depth region corresponding to maximum displacement damage.[21] We have since found this phenomenon to occur generally for all of the dopants commonly used in silicon,[22] and Morehead has shown mathematically that it should occur for any defect-controlled impurity diffusion process, as a consequence of the gradient in diffusivity.[23]

Figure 9(b) shows the carrier concentration profile of a 0.01-Ω cm arsenic-doped ⟨100⟩ silicon wafer that was bombarded with 150-keV protons for 1 h at 700 °C and at a flux of 3.5×10^{13} protons/cm^2 s. This profile was measured by spreading resistance after a half-hour post-bombardment anneal at 900 °C in an argon atomosphere to ensure that the arsenic dopant would be electrically active. The indicated dopant rejection at 1.2 μm, with an accompanying pileup a few tenths of a μm on either side of this depth region, illustrates the behavior observed for similar proton bombardments of wafers that had been doped homogeneously with arsenic, antimony, phosphorus, boron, or gallium. The magnitude of the profile dip, as measured by spreading resistance, appears exaggerated by comparison with the total impurity profiles obtained by neutron activation ion channeling, or secondary-ion mass spectroscopy. The depth position of the dip, however, is well reproduced by the various profiling methods, and agrees well with the channeled ion channeling measurements of maximum disorder depth.

IV. RESULTS AND DISCUSSION

The damage profiles obtained by the channeling method and the resistivity R_D and hydrogen profile R_p obtained by nuclear reaction are given in Table I. Standard deviations ΔR_D, ΔR_p are obtained from the FWHM divided by 2.355. Small corrections to the detector resolution and to energy straggling of helium ions in silicon reduce the extracted ΔR_D by 3%–5%. The uncertainty and the standard deviation of the mean projected depth are estimated from the uncertainty in the energy loss of helium ions in silicon, and from the reproducibility of the profile extracted from the channeling measurement. The ±5% uncertainty in R_D in the spreading-resistance measurement is due mainly to the positioning of the probe on the shallow beveled surface.

TABLE I. R_p and ΔR_p of protons in silicon. (Rigorously speaking, the damage profile gives R_D, not R_p; however, since the profiles are identical, no distinction between R_p and R_D will be made in the present case.)

Method	Proton energy (keV)	Mean projected range (Å)	Standard deviation (Å)
Channeling	50(1)	5 000(250)	400(50)
	75(1)	6 300(300)	480(50)
	85(1)	7 200(350)	520(50)
	100(1)	8 550(450)	580(60)
	125(1)	10 200(500)	610(60)
	150(1)	12 000(600)	720(70)
	175(1)	14 700(750)	750(80)
	200(2)	17 300(850)	840(90)
	225(2)	20 000(1000)	900(90)
	250(2)	22 700(1200)	1000(100)
Nuclear reaction	75(1)	6 000(···)	460(···)
	48(1)	4 700(···)	460(···)
Resistivity	150	12 500(±5%)	···
	300	27 800(±5%)	···
	375	36 300(±5%)	···
	450	48 700(±5%)	···

The projected range R_p and the measured damage depth R_D are given in Fig. 10. Our measurements are complementary to other measurements, such as those of Ligeon and Guivarc'h, Thompson and Robinson, and Baruch *et al.*[7] The curve for projected range versus energy, calculated by Gibbons *et al.*,[24] is also given in Fig. 10. At low energy, the calculation overestimates R_p. The reason may be that Northcliffe and Schilling's tabulation[25] on energy loss is used in the calculation by Gibbons *et al.*[24]; any error in proton energy loss will be reflected in the calculated value of R_p.

At 50 keV, the value given by Northcliffe and Schilling[25] for electronic energy loss of protons in silicon agrees with those obtained by the LSS calculation; at 10 keV, it is 10% higher. As Thompson and Robinson pointed out,[5] the electronic energy loss calculated by the LSS method has to be increased by 60% in order to fit their damage distribution in the 10–40-keV region. From the present measurements it appears that Northcliffe and Schilling[25] too underestimate the proton energy loss in silicon at low energies but overestimate it at high energies. Our results at high energies connect well with those of Marcinkowski *et al.*[26] From their measurement of proton energy loss in silicon, they obtained a range vs energy relation of 0.8–2 MeV as $R = AE^x$ for curve fit parameters $A = 16.41$ and $x = 1.64$; here R is expressed in μm and energy in MeV. Our R_p results

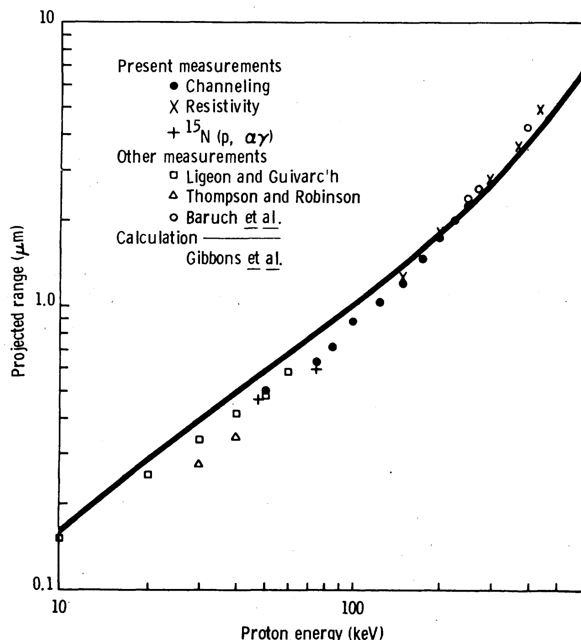

FIG. 10. Comparison of present depth measurements to others. Channeling measurements (●), spreading resistivity (×) gives damage profile, and nuclear reaction (+) gives hydrogen project range. Measurements by Ligeon and Guivarc'h (□), Thompson and Robinson (Δ), and Baruch *et al*. (○) are also given; they are in good agreement with our measurements. The solid curve is the calculation by Gibbons *et al*. using Northcliffe and Schilling's energy-loss value.

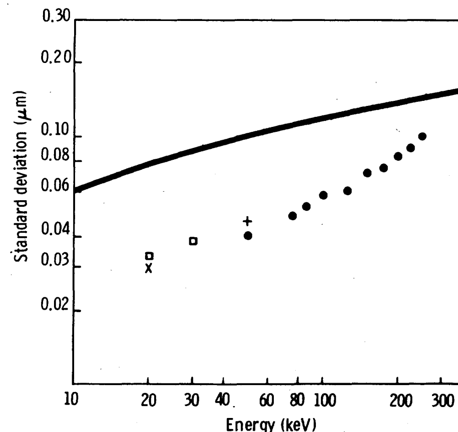

FIG. 11. Standard deviation of measured profiles is considerably lower than the theoretical calculation by Gibbons *et al*. The notations are the same as in Fig. 10.

are in good agreement with a recent compilation by Andersen and Ziegler.[27]

Figure 11 gives the standard deviation versus proton energy. Our results indicate that there is no difference between the damage profile and the hydrogen profile. This finding is in good agreement with the observations of Ligeon and Guivarc'h.[6] For light projectiles in heavy targets, where the amount of recoil damage is negligible, one would expect that $R_D \rightarrow R_p$ and $\Delta R_D \rightarrow \Delta R_p$.

Alternatively, one can assume that though the hydrogen range actually is somewhat different from the damage distribution, the hydrogen atoms may have moved towards the vacancy-rich layer and become trapped at the damage region. This migration induced by damage stress[28] could explain why the measured hydrogen and damage profiles are identical.

As for the amount of damage, Fig. 4 has indicated that the defect formation for a broad temperature range is equivalent to 8–9 silicon atoms permanently displaced from the lattice site per incident proton. This number is independent of energy, because most of the damage is due to nuclear collision between protons and silicon atoms. The electronic stopping of protons in silicon does not produce enough silicon displacement to be measurable by channeling.

In the present study, the number of equivalent silicon atoms displaced per incident proton is independent of proton dose between 1×10^{16} and 8×10^{16} protons/cm^2. For doses below 10^{16}/cm^2, it is difficult to measure the small amount of damage done by channeling. For doses above 8×10^{16}/cm^2, damage reaches saturation level; for over 10^{17}/cm^2, the silicon becomes amorphized.

The range distribution and the damage distribution are considerably narrower than is predicted by Gibbons *et al*.[24] Much of the discrepancy arises, we believe, because the theoretical calculation made with Northcliffe and Schilling's tabulation gives an underestimate of the electronic energy loss of protons in silicon. This underestimate reflects the larger calculated R_p (Fig. 10) and consequently an even larger calculated range distribution, as is seen in Fig. 11. This observation was also made by Thompson and Robinson.[5] To make their Monte Carlo calculation match their damage measurement, they have to assume an electronic energy loss 60% above that obtained by application of the LSS theory.

Another probable reason why the range and damage distributions are narrow is that the nuclear stopping power is lower than is predicted by most of the theories.[29] Our present measurement probably contributes some support to the claim made by Kalbitzer *et al.* in Ref. 29.

V. CONCLUSIONS

(i) Profiles of damage due to protons implanted in silicon at 50–250 keV can be obtained by backscattering and channeling. (ii) These profiles

can be confirmed by spreading-resistance measurement, by enhanced diffusion measurement, and by hydrogen profiles measured by the $^{15}N(p,\alpha)^{12}C$ nuclear reaction. (iii) Measured damage profiles agree with the hydrogen profile obtained in our measurement. (iv) The total amount of damage is equivalent to 9 silicon atoms displaced per incident proton at 50 keV and 100–400 °C. (v) The total amount of damage, its distribution, and the amount of dechanneling have also been studied as a function of ambient temperature between −170 and +600 °C. (vi) The present measurements are in good agreement with published range and damage data. (vii) At 200 keV, the depth measurement agrees with existing calculations; at 50 keV, it is 20% below the theoretical calculation. (viii) The depth distribution is 30%–60% narrower than the theoretical calculation.

ACKNOWLEDGMENTS

We are indebted to W. A. Lanford, J. F. Ziegler, and J. Keller for their hydrogen profiling (Fig. 7) done at Wright Nuclear Structure Laboratory, Yale University. We also thank E. F. Gorey for his spreading-resistance measurements and D. J. Faoro for his assistance in the hydrogen implantation.

---

[1] *Application of Ion Beams to Metals*, edited by S. T. Picraux, E. P. EerNisse, and F. L. Vook (Plenum, New York, 1973).

[2] Proceedings of the International Conference at Warwick, England, 1975 (unpublished).

[3] Several papers cover this subject—for example, P. Baruch, C. Constantin, J. C. Pfister, and R. Saint-esprit, Discuss. Faraday Soc. 31, 76 (1961); D. G. Nelson, J. F. Gibbons, and W. S. Johnson, Appl. Phys. Lett. 15, 246 (1969); Y. Ohmura, S. Mimura, M. Kanazawa, T. Abe, and M. Konaka, Radiat. Eff. 15, 167 (1972).

[4] For example, Y. Ohmura, Y. Zohta, and M. Kanazawa, Solid State Commun. 11, 263 (1972).

[5] D. A. Thompson and J. E. Robinson, Nucl. Instrum. Methods 131, 261 (1976).

[6] E. Ligeon and A. Guivarc'h, Radiat. Eff. 27, 129 (1976).

[7] W. K. Chu, R. H. Kastl, R. F. Lever, S. Mader, and B. J. Masters, in Proceedings of the Fifth International Conference on Ion Implantation in Semiconductors and Other Materials, Boulder, Colorado, 1976 (unpublished).

[8] F. Ajzenberg-Selove and T. Lauritsen, Nucl. Phys. A 114, 1 (1968).

[9] F. Ajzenberg-Selove, Nucl. Phys. A 152, 1 (1970).

[10] J. B. Marion, Rev. Mod. Phys. 38, 660 (1966).

[11] J. F. Ziegler, J. Appl. Phys. 43, 2973 (1972).

[12] D. Schmid, Radiat. Eff. 17, 201 (1973).

[13] E. Bøgh, Can. J. Phys. 46, 653 (1968).

[14] J. F. Ziegler and W. K. Chu, Atomic Data and Nucl. Data Tables 13, 463 (1974).

[15] Y. Quere, Radiat. Eff. 38, 253 (1976).

[16] H. J. Stein, J. Electron. Mater. 4, 159 (1975).

[17] W. A. Lanford, H. P. Trautvetter, J. F. Ziegler, and J. Keller, Appl. Phys. Lett. 28, 566 (1976).

[18] P. Baruch, J. Monnier, B. Blanchard, and C. Castaing, Appl. Phys. Lett. 26, 77 (1975).

[19] G. H. Schwuttke, K. Brack, and E. F. Gorey, in *Ion Implantation*, edited by F. H. Eisen and L. T. Chadderton (Gordon and Breach, New York, 1971), p. 139.

[20] Y. Ohmura, Y. Zohta, and M. Kanazawa, Phys. Status Solidi A 15, 93 (1973).

[21] P. Baruch, J. Monnier, B. Blanchard, and C. Castaing, in *Ion Implantation in Semiconductors*, edited by S. Namba (Plenum, New York, 1975), p. 189; and in *Lattice Defects in Semiconductors, 1974* (Institute of Physics, London, 1975), p. 453.

[22] B. Masters, E. F. Gorey, R. H. Kastl, W. K. Chu, and R. F. Lever (unpublished).

[23] F. Morehead, Appl. Phys. Lett (to be published).

[24] J. F. Gibbons, W. S. Johnson, and S. W. Mylroie, *Projected Range Statistics, Semiconductor and Related Materials*, 2nd ed. (Halstead, New York, 1976).

[25] L. C. Northcliffe and R. F. Schilling, Nucl. Data Tables A 7, 233 (1970).

[26] A. Marcinkowski, H. Rzewuski, and Z. Werner, Nucl. Instrum. Methods 57, 338 (1967).

[27] H. H. Andersen and J. F. Ziegler (unpublished).

[28] G. Dearnaley, Appl. Phys. Lett. 28, 244 (1976).

[29] S. Kalbitzer, H. Oetzmann, H. Grahmann, and A. Feuerstein, Z. Phys. A 278, 223 (1976).

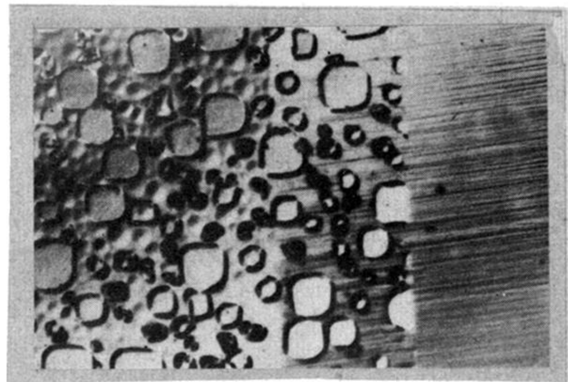

FIG. 8. Optical microscope view, showing the circular gas bubbles or blisters formed by high-dose proton bombardment in silicon, and the almost square craters that result from blister eruption in a ⟨100⟩ specimen. Magnification 700×. The crater depth can be determined from the length measurement and the beveling angle.